

# Assembling of three-dimensional crystals by optical depletion force induced by a single focused laser beam

Hai-Dong Deng,<sup>1,2</sup> Guang-Can Li,<sup>1</sup> Hai-Ying Liu,<sup>1</sup> Qiao-Feng Dai,<sup>1</sup> Li-Jun Wu,<sup>1</sup> Sheng Lan,<sup>1,\*</sup> Achanta Venu Gopal,<sup>3</sup> Vyacheslav A. Trofimov,<sup>4</sup> and Tatiana M. Lysak<sup>4</sup>

<sup>1</sup>Laboratory of Nanophotonic Functional Materials and Devices, School of Information and Optoelectronic Science and Engineering, South China Normal University, Guangzhou 510006, China

<sup>2</sup>College of Science, South China Agricultural University, Guangzhou, Guangdong 510642, China

<sup>3</sup>Department of Condensed Matter Physics and Material Science, Tata Institute of Fundamental Research, Homi Bhabha Road, Mumbai 400005, India

<sup>4</sup>Department of Computational Mathematics and Cybernetics, M. V. Lomonosov Moscow State University, Moscow 119992, Russia

\*slan@scnu.edu.cn

**Abstract:** We proposed a method to assemble microspheres into a three-dimensional crystal by utilizing the giant nonequilibrium depletion force produced by nanoparticles. Such assembling was demonstrated in a colloid formed by suitably mixing silica microspheres and magnetic nanoparticles. The giant nonequilibrium depletion force was generated by quickly driving magnetic nanoparticles out of the focusing region of a laser light through both optical force and thermophoresis. The thermophoretic binding of silica beads is so tight that a colloidal photonic crystal can be achieved after complete evaporation of solvent. This technique could be employed for fabrication of colloidal photonic crystals and molecular sieves.

©2012 Optical Society of America

**OCIS codes:** (350.5340) Photothermal effects; (350.4855) Optical tweezers or optical manipulation; (350.4238) Nanophotonics and photonic crystals.

---

## References and links

1. N. A. Clark, A. J. Hurd, and B. J. Ackerson, "Single colloidal crystal," *Nature* **281**(5726), 57–60 (1979).
2. Y. Zeng and D. J. Harrison, "Self-assembled colloidal arrays as three-dimensional nanofluidic sieves for separation of biomolecules on microchips," *Anal. Chem.* **79**(6), 2289–2295 (2007).
3. M. S. Thijssen, R. Sprik, J. E. G. J. Wijnhoven, M. Megens, T. Narayanan, A. Lagendijk, and W. L. Vos, "Inhibited Light Propagation and Broadband Reflection in Photonic Air-Sphere Crystals," *Phys. Rev. Lett.* **83**(14), 2730–2733 (1999).
4. J. H. Holtz and S. A. Asher, "Polymerized colloidal crystal hydrogel films as intelligent chemical sensing materials," *Nature* **389**(6653), 829–832 (1997).
5. R. W. J. Scott, S. M. Yang, G. Chabanis, N. Coombs, D. E. Williams, and G. A. Ozin, "Tin Dioxide Opals and Inverted Opals: Near-Ideal Microstructures for Gas Sensors," *Adv. Mater. (Deerfield Beach Fla.)* **13**(19), 1468–1472 (2001).
6. P. N. Pusey and W. van Megen, "Phase behaviour of concentrated suspensions of nearly hard colloidal spheres," *Nature* **320**(6060), 340–342 (1986).
7. M. Trau, D. A. Saville, and I. A. Aksay, "Field-Induced Layering of Colloidal Crystals," *Science* **272**(5262), 706–709 (1996).
8. P. Sheng, W. Wen, N. Wang, H. Ma, Z. Lin, W. Y. Zhang, X. Y. Lei, Z. L. Wang, D. G. Zheng, W. Y. Tam, and C. T. Chan, "Multiply coated microspheres. A platform for realizing fields-induced structural transition and photonic bandgap," *Pure Appl. Chem.* **72**(1-2), 309–315 (2000).
9. P. T. Korda and D. G. Grier, "Annealing thin colloidal crystals with optical gradient forces," *J. Chem. Phys.* **114**(17), 7570–7573 (2001).
10. S. H. Park, D. Qin, and Y. Xia, "Crystallization of Mesoscale Particles over Large Areas," *Adv. Mater. (Deerfield Beach Fla.)* **10**(13), 1028–1032 (1998).
11. A. van Blaaderen and P. Wiltzius, "Growing large, well-oriented colloidal crystals," *Adv. Mater. (Deerfield Beach Fla.)* **9**(10), 833–835 (1997).
12. B. Hatton, L. Mishchenko, S. Davis, K. H. Sandhage, and J. Aizenberg, "Assembly of large-area, highly ordered, crack-free inverse opal films," *Proc. Natl. Acad. Sci. U.S.A.* **107**(23), 10354–10359 (2010).
13. P. Jiang and M. J. McFarland, "Large-scale fabrication of wafer-size colloidal crystals, macroporous polymers and nanocomposites by spin-coating," *J. Am. Chem. Soc.* **126**(42), 13778–13786 (2004).

14. N. Aubry, P. Singh, M. Janjua, and S. Nudurupati, "Micro- and nanoparticles self-assembly for virtually defect-free, adjustable monolayers," *Proc. Natl. Acad. Sci. U.S.A.* **105**(10), 3711–3714 (2008).
15. S. Duhr and D. Braun, "Two-dimensional colloidal crystals formed by thermophoresis and convection," *Appl. Phys. Lett.* **86**(13), 131921 (2005).
16. D. Braun and A. Libchaber, "Trapping of DNA by thermophoretic depletion and convection," *Phys. Rev. Lett.* **89**(18), 188103 (2002).
17. P. Baaske, F. M. Weinert, S. Duhr, K. H. Lemke, M. J. Russell, and D. Braun, "Extreme accumulation of nucleotides in simulated hydrothermal pore systems," *Proc. Natl. Acad. Sci. U.S.A.* **104**(22), 9346–9351 (2007).
18. F. M. Weinert and D. Braun, "Observation of slip flow in thermophoresis," *Phys. Rev. Lett.* **101**(16), 168301 (2008).
19. H. R. Jiang, H. Wada, N. Yoshinaga, and M. Sano, "Manipulation of colloids by a nonequilibrium depletion force in a temperature gradient," *Phys. Rev. Lett.* **102**(20), 208301 (2009).
20. Z. M. Meng, H. Y. Liu, W. R. Zhao, W. Zhang, H. D. Deng, Q. F. Dai, L. J. Wu, S. Lan, and A. V. Gopal, "Effects of optical forces on the transmission of magnetic fluids investigated by Z-scan technique," *J. Appl. Phys.* **106**(4), 044905 (2009).
21. R. Piazza and A. Guarino, "Soret effect in interacting micellar solutions," *Phys. Rev. Lett.* **88**(20), 208302 (2002).
22. J. C. Crocker, J. A. Matteo, A. D. Dinsmore, and A. G. Yodh, "Entropic Attraction and Repulsion in Binary Colloids Probed with a Line Optical Tweezer," *Phys. Rev. Lett.* **82**(21), 4352–4355 (1999).
23. Q. F. Dai, H. Y. Liu, J. Liu, L. J. Wu, Q. Guo, W. Hu, X. B. Yang, S. H. Liu, S. Lan, A. V. Gopal, and V. A. Trofimov, "Self-induced transparency in colloidal liquids by Z-scan-based optical trapping," *Appl. Phys. Lett.* **92**(15), 153111 (2008).
24. J. Liu, Q. F. Dai, Z. M. Meng, X. G. Huang, L. J. Wu, Q. Guo, W. Hu, S. Lan, A. V. Gopal, and V. A. Trofimov, "All-optical switching using controlled formation of large volume three-dimensional optical matter," *Appl. Phys. Lett.* **92**(23), 233108 (2008).
25. J. Liu, Q. F. Dai, X. G. Huang, L. J. Wu, Q. Guo, W. Hu, X. B. Yang, S. Lan, A. V. Gopal, and V. A. Trofimov, "Dynamics of optical matter creation and annihilation in colloidal liquids controlled by laser trapping power," *Opt. Lett.* **33**(22), 2617–2619 (2008).

## 1. Introduction

Periodic structures are of interest for photonic, plasmonic and other studies. As top-down approaches are expensive, bottom-up approaches like formation of colloidal crystals in diluted solution are pursued [1]. These have been used to realize molecular sieves [2], photonic crystals (PCs) [3], and chemical sensors [4,5]. Particularly, monodispersed microspheres were self-assembled into colloidal crystals by methods that rely on different mechanisms [6–11]. Each technique has its own advantages and limitations. For example, colloidal crystals with very few defects and dislocations can be obtained by using capillary force [12]. However, it usually takes a long time (generally several hours) to assemble the crystals. In contrast, the assembling based on spin coating is a time-effective technique to fabricate colloidal crystals with large sizes but the controlling of defects and dislocations remains to be a problem [13]. In the cases when the size of colloidal crystals is not a primary consideration, a time-effective fabrication technique that renders high-quality colloidal crystals with few defects and dislocations becomes important. For this reason, techniques based on phoretic movement have attracted much attention in the past decade. Among these techniques, electrophoresis based monolayer assembly has been reported recently [14]. Similarly, thermophoresis mediated assembly of two-dimensional crystals and accumulation of biomolecules were also demonstrated [15–17]. However, the thermal gradient and/or the Soret coefficient (that governs the thermophoretic motion) required are quite large to move bigger and heavier particles. Thus, particle assembly due to thermophoresis requires an additional support mechanism.

In general,  $S_T \nabla T = \beta f$  where  $\beta$  is  $1/k_B T$  and  $f$  is the net force acting on the particle due to thermal gradient and thus for movement of heavier particles, like silica beads, large Soret coefficient ( $S_T$ ) and/or temperature gradient ( $\nabla T$ ) is required. For large temperature gradient, satisfying the condition,  $\nabla T > D/aD_T$  where  $D$  and  $D_T$  are the diffusion and thermal diffusion coefficients and  $a$  is the hydrodynamic radius of the particle, Marangoni-like slip flow leads to movement of particles to the colder surface [18]. While the longitudinal component of the velocity is zero, the transverse component (that is parallel to the surface) is non-zero resulting in the slip flow related movement and attraction of positive Soret coefficient particles to each

other on the colder surface. Experimentally, it is difficult to realize required large  $\nabla T$ . Thus, ways to control  $S_T$  is important for both enhancement as well as having selective accumulation of particles. Recently, it has been shown that the effective Soret coefficient  $S_T^*$  of polystyrene (PS) beads in a colloidal suspension can be tuned, by changing the polymer concentration in the solution, to negative values [19].

In this article, we propose a method to assemble microspheres into a three-dimensional (3D) crystal by utilizing the giant nonequilibrium depletion force produced by nanoparticles. Such assembly was demonstrated in a colloid formed by suitably mixing silica or PS beads with  $\text{Fe}_3\text{O}_4$  nanoparticles (hereafter referred to as magnetic nanoparticles). Apart from the thermophoresis of magnetic nanoparticles induced by a laser light, the large absorption force that drives magnetic nanoparticles quickly out of the focus play a crucial role in generating the giant nonequilibrium force. The resulting nonequilibrium distribution in the concentration of magnetic nanoparticles leads to an initial diffusiophoretic followed by thermophoretic motion of silica beads to the focus or heating center with a large effective Soret coefficient  $S_T^*$ , forming a 3D crystal with few defects and dislocations. The thermophoretic binding of silica beads is so tight that a colloidal PC can be achieved after complete evaporation of solvent.

## 2. Sample preparation and experimental details

The aqueous solution of silica beads used in our experiments were purchased from Duke Scientific Corporation. The diameter of silica beads is 1.6  $\mu\text{m}$  and they are uniformly dispersed in water with a volume fraction of 10%. The water-based magnetic fluid we used was prepared by Central Iron and Steel Research Institute, China. The average diameter of magnetic nanoparticles was determined to be  $\sim 12$  nm and the weight fraction of magnetic nanoparticles was measured to be 25.7%. In our experiments, the magnetic fluid was first diluted with water to magnetic fluids with different volume densities of magnetic nanoparticles. Then, the aqueous solution of silica beads was mixed with these magnetic fluids at a volume ratio of 3: 1 and sonicated for half an hour to obtain new colloids with uniformly distributed silica beads and magnetic nanoparticles for assembling experiments. This procedure ensures almost the same number density of silica beads in all colloids. Then, the new colloids were sealed into sample cells with a thickness of about 50  $\mu\text{m}$ . Each sample cell was formed by two glass cover slides. The 532-nm light from a solid-state laser (Verdi-5, Coherent) was focused on the sample cell by using a 63 $\times$  objective lens (NA = 1.43), as schematically shown in Fig. 1(a). The spot size of the laser beam on the sample cell is similar to the diameter of silica beads. It is important to place the focus of the laser light just above the bottom wall of the sample cell. To do so, the absorption force, which is much larger than the gradient force [20], will push magnetic nanoparticles out of the focus. It was found that a depletion region of magnetic nanoparticles could be easily created at the focus by utilizing the large absorption force and an effective assembling of silica beads could be realized. The assembling process of silica beads was monitored by using an inverted microscope (Axio Observer A1, Zeiss) in combination with a charge-coupled device (CCD).

## 3. Results and discussion

### 3.1 Layer by layer formation of 3D crystals

Initially, the heavier silica beads were observed to settle on the bottom wall of the sample cell. Once the laser beam was focused into the sample cell, a fast movement of silica beads towards the focus was clearly observed. By particle tracking, we measured that the average velocity of particles varies from about 150  $\mu\text{m}/\text{min}$  in the first 15 seconds to 75  $\mu\text{m}/\text{min}$  in the next 15 seconds. The 2D crystal grew up very quickly and more than 40 silica beads were found along the diameter of the circular-shaped crystal after about 60 seconds. Silica beads in the 2D crystal were regularly and closely packed into a hexagonal lattice with negligible defects. Also, it should be emphasized that a very low laser power of only about 15 mW was needed to trigger the assembling of silica beads. The role of absorption force and

thermophoresis may be understood as the assembly did not occur when an 800-nm light is used due to weak absorption in magnetic nanoparticles.

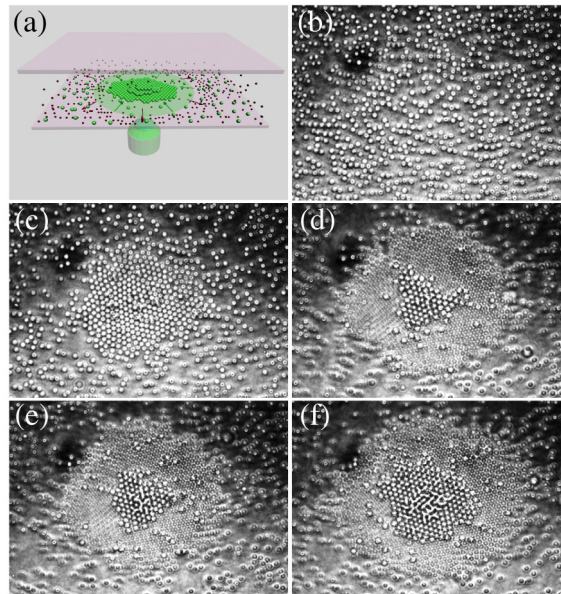


Fig. 1. (a) Schematic showing the assembling process in a sealed glass cell. Big spheres in green color represent silica beads while small spheres in violet color represent magnetic nanoparticles. The moving directions of silica beads and magnetic nanoparticles are indicated by green and violet arrows, respectively. (b-f) are CCD images showing different stages in the formation of the 3D crystal.

During the assembling process, a closer look at the 2D crystal revealed that some silica beads accumulated at the edge of the 2D crystal climbed up onto the crystal and moved towards the central region with a slower speed. This resulted in forming of a second layer of closely packed silica beads at the central region on top of the first one. Although the area of the second layer of silica beads was much smaller than the first one, this layer-by-layer crystallization process continued. The CCD images illustrating the assembling process of silica beads through a layer-by-layer fashion into a 3D crystal are presented in Fig. 1. In the optimum case, a 3D crystal with five layers of regularly packed silica beads was obtained, as shown in Fig. 2. Apart from the observation through the microscope with CCD, the laser light also acted as a probe for the ordering of the formed crystal. The evolution of the diffraction pattern of the incident light, from a uniform Gaussian distribution to a Debye-Scherrer ring and eventually to Bragg diffraction spots, during the assembling process shown in Fig. 3 clearly indicates the formation of an ordered structure.

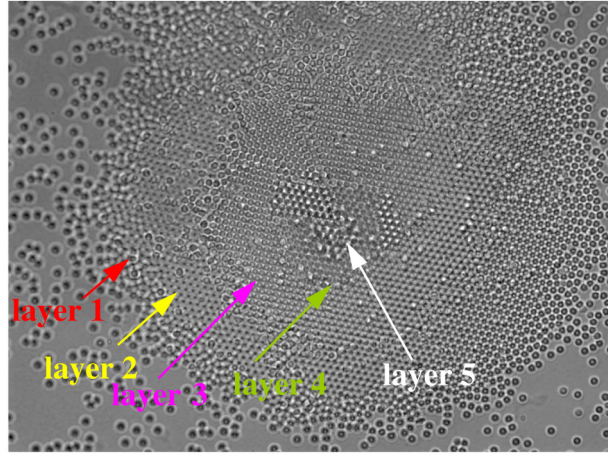


Fig. 2. CCD image of a 3D crystal with five layers of regularly packed silica beads.

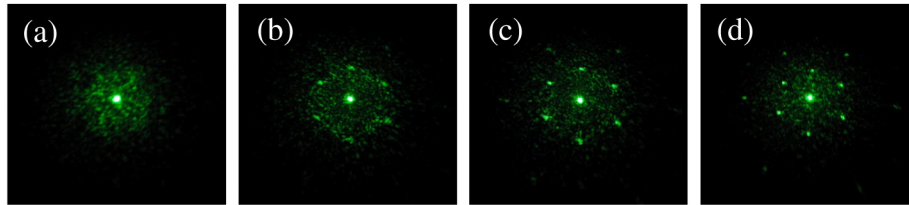


Fig. 3. Evolution of the diffraction pattern during the assembling process of the crystal.

### 3.2 Effect of ratio of magnetic to silica particles in the colloid

By using colloids with different number densities of magnetic nanoparticles, it was found that the largest and best 3D crystals were obtained when the number density of magnetic particles was chosen to be  $\sim 1.75 \times 10^{16} \text{ cm}^{-3}$ . In this case, the colloid was obtained by mixing the aqueous solution of silica beads with the magnetic fluid at a weight ratio of 3: 1. This phenomenon can be interpreted by the effective Soret coefficient of silica beads that is dependent on the concentration of magnetic nanoparticles. Basically, the effective Soret coefficient of silica beads can be expressed as [19]

$$S_T^* = S_T^b - 2\pi(S_T^m - \frac{1}{T})a\lambda^2 c_m. \quad (1)$$

Here,  $S_T^b$  and  $S_T^m$  are the Soret coefficients of silica beads and magnetic nanoparticles,  $a$  is the radius of silica beads,  $\lambda$  is the interaction distance between the two types of particles, and  $c_m$  is the concentration (or the number density) of magnetic nanoparticles at the center of the focus in the steady state. From Eq. (1), it can be seen that the effective Soret coefficient of silica beads increases linearly with the equilibrium concentration of magnetic nanoparticles at the beam center  $c_m$  that increases with the background concentration of magnetic nanoparticles. Accordingly, it was found that the assembling speed became faster with increasing concentration of magnetic nanoparticles, leading to a larger size and better quality of the formed crystal. Once the concentration of magnetic nanoparticles exceeds a certain value (i.e.,  $c_m \sim 1.75 \times 10^{16} \text{ cm}^{-3}$  in our case), however, we observed a slowdown of the assembly and a reduction in the crystal size. It implies a decrease of the effective Soret coefficient of silica beads. In fact, the effective Soret coefficient generally depends on the concentration of the particles (both magnetic and silica beads). Though the Soret coefficient can be considered as a constant when the particle concentration is low, in the case of high concentration, the interaction between particles cannot be neglected and the Soret coefficient

decreases rapidly with increasing concentration [21]. Therefore, the effective Soret coefficient of silica beads begins to decrease when the concentration of magnetic nanoparticles exceeds a certain value. The 3D crystals obtained by using colloids with different number densities of magnetic particles are compared in Fig. 4.

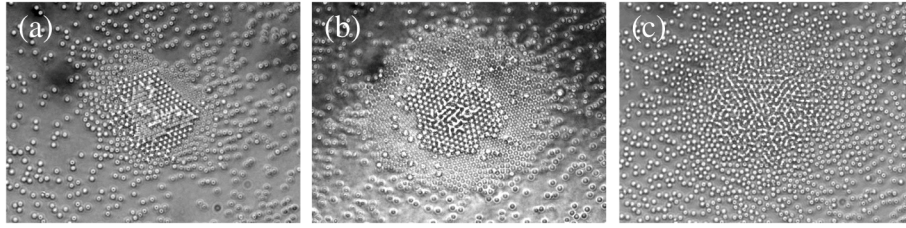


Fig. 4. 3D structures obtained by using colloids with similar number densities of silica beads ( $c_b$ ) and different number densities of magnetic nanoparticles ( $c_m$ ). (a)  $c_b = 3.14 \times 10^9 \text{ cm}^{-3}$ ,  $c_m = 2.38 \times 10^{16} \text{ cm}^{-3}$ ; (b)  $c_b = 3.40 \times 10^9 \text{ cm}^{-3}$ ,  $c_m = 1.75 \times 10^{16} \text{ cm}^{-3}$  and (c)  $c_b = 3.23 \times 10^9 \text{ cm}^{-3}$ ,  $c_m = 4.20 \times 10^{15} \text{ cm}^{-3}$ .

### 3.3 Effect of particle size and type of particles

Apart from the concentration of magnetic nanoparticles, it is apparent from Eq. (1) that another quantity that significantly affects the effective Soret coefficient of silica beads is their own Soret coefficient ( $S_T^b$ ). It has been known that the Soret coefficient of particles scales linearly with the size of particles. We have performed assembling experiments by using silica beads with a smaller diameter of 0.70  $\mu\text{m}$ . In this case, a smaller effective Soret coefficient as well as a stronger Brownian motion is expected. On the other hand, the interaction between 0.7- $\mu\text{m}$  silica beads and magnetic nanoparticles is thought to be weaker as compared with 1.6- $\mu\text{m}$  silica beads [22], leading to a weaker nonequilibrium depletion force. Accordingly, it was found that only a 2D crystal with a smaller size could be obtained. Also, the assembling of PS beads with a similar diameter (1.9  $\mu\text{m}$ ) but a positive Soret coefficient [19] has been carried out wherein a 3D crystal but with a smaller size was achieved. However, the 3D crystal was formed on the top wall of the sample cell. In addition, the laser power necessary to realize the assembly increased dramatically to about 200 mW due to the positive Soret coefficient. In this case the role of radiation force also comes into picture due to lighter particles and large intensity used. The 2D and 3D crystals formed by using smaller silica beads and PS beads are shown in Figs. 5(a) and 5(b), respectively.

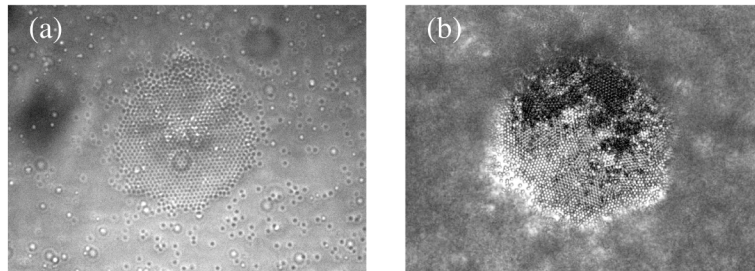


Fig. 5. Images of the 2D crystal formed with 0.7- $\mu\text{m}$  silica beads (a) and the 3D crystal formed with 1.9- $\mu\text{m}$  PS beads (b).

### 3.4 Crystallization on glass slides

The assembling experiments described above were carried out in sample cells where the light scattering from suspended particles and walls of the cell also contribute to the formation of colloidal crystal like in optical matter. Previously, we have reported several techniques based on optical forces to fabricate optical matters and the creation and annihilation dynamics of

optical matters [23–25]. In these cases, the fabricated optical matters will be destroyed by the Brownian motion once the laser beam was blocked. Similarly, the optical matter formed by nonequilibrium depletion force will eventually be destroyed by the Brownian motion of particles once the laser beam is turned off. To avoid effects of shape of the cell on the assembling process as well as to get usable structures for OPAL or inverse OPAL like structures and molecular sieves, we wanted to check if the assembling process could be replicated on a glass slide.

For this, a droplet of the colloid containing both silica beads and magnetic nanoparticles was placed on the surface of a glass slide and the laser beam was focused on the surface of the glass slide. In this case, one would expect free convection. Indeed, during the initial period the liquid flow is not significant or noticeable. However, as the time progresses crystallization takes place and water gets heated due to conduction. As the water temperature increases, convection sets in and we see bifurcation in the flow. Eventually, the liquid evaporated and the volume of the colloidal droplet reduced with time. Just before water in the droplet was completely evaporated, the silica beads in the crystal suffer from strong force that tends to break the crystal. However, the tight binding between the particles seems to prevent the crystal from being destroyed, leaving a perfect colloidal PC on the surface of the glass slide. Since the colloidal PC was covered by magnetic nanoparticles, the sample was baked at 100°C for several minutes to partially remove the magnetic nanoparticles. In Fig. 6, the CCD and SEM images and diffraction pattern of the crystal are shown. Three layers of silica beads that are regularly arranged in a hexagonal lattice can be identified in the colloidal PC. In Fig. 6(c), only three silica beads were observed in the top layer because most silica beads in this layer had been removed with the magnetic nanoparticles coated by surface surfactant. Therefore, this technique offers us an easy, fast, and effective way of fabricating colloidal PCs, especially for those composed of both micro- and nanoparticles.

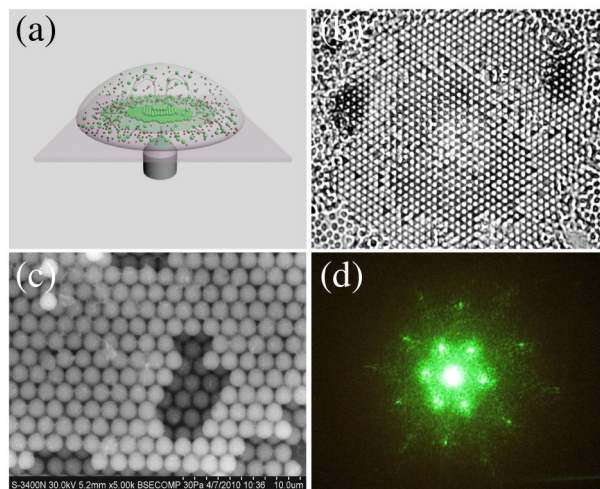


Fig. 6. Shown are (a) the schematic of the experiment, (b) CCD and (c) SEM images of the 3D colloidal PC, and (d) diffraction pattern of the incident light showing crystallinity of the assembled microspheres.

#### 4. Summary

We have proposed and demonstrated a technique to assemble silica beads into a 3D crystal with few defects and dislocations by utilizing the giant nonequilibrium depletion force produced by magnetic nanoparticles. Furthermore, the tight binding of silica beads makes it possible to obtain 3D colloidal PCs after the complete evaporation of water. This phenomenon can be employed as a low cost and faster fabrication technique for high-quality 3D colloidal PCs. In addition, the control and enhancement of effective Soret coefficient

shown in this work could be useful for various applications in widely varying fields of science.

### **Acknowledgments**

The authors acknowledge the financial support from the National Natural Science Foundation of China (Grant Nos. 10974060, 51171066 and 11111120068) and the program for high-level professionals in the universities of Guangdong province, China.